Science
AAAS

A Cellular Framework for Gut-Looping Morphogenesis in Zebrafish

Sally Horne-Badovinac, *et al.*

Science **302**, 662 (2003);
DOI: 10.1126/science.1085397

Science (print ISSN 0036-8075; online ISSN 1095-9203) is published weekly, except the last week in December, by the American Association for the Advancement of Science, 1200 New York Avenue NW, Washington, DC 20005.

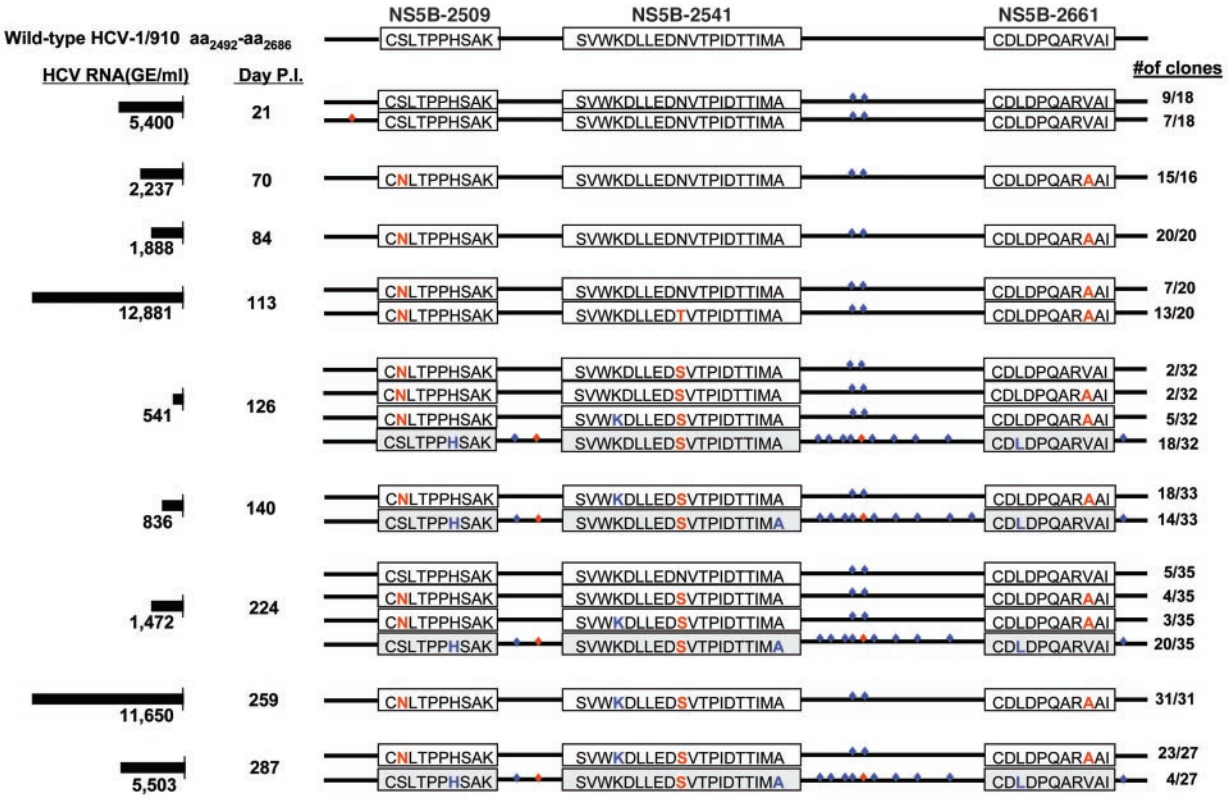

Fig. 4. Evolution of three class I MHC-restricted epitopes in the HCV NS5B protein (*28*). A 585-nucleotide region of HCV NS5B containing the NS5B-2509, NS5B-2541, and NS5B-2661 epitopes was amplified with the use of nested RT-PCR primers from the plasma of CBO627 (*22*). The boxed regions indicate $CD8^+$ T cell epitopes. Missense mutations resulting in amino acid changes within the epitopes are shown in red; silent mutations, in blue. The red diamonds reflect missense mutations in the flanking regions, and the blue diamonds indicate silent mutations. The number of clones with the indicated sequence and the total number of clones examined are shown on the right. In some cases, minor populations with an additional silent mutation were identified (days 21, 70, 126, 140, and 224) but are not shown for clarity. P.I., postinfection.

13. G. Missale *et al.*, *J. Clin. Invest.* **98**, 706 (1996).
14. H. M. Diepolder *et al.*, *Lancet* **346**, 1006 (1995).
15. J. T. Gerlach *et al.*, *Gastroenterology* **117**, 933 (1999).
16. R. Thimme *et al.*, *Proc. Natl. Acad. Sci. U.S.A.* **99**, 15661 (2002).
17. Q. L. Choo *et al.*, *Science* **224**, 359 (1989).
18. C. M. Walker *et al.*, unpublished observations.
19. S. A. Kalams, B. D. Walker, *J. Exp. Med.* **188**, 2199 (1998).
20. J. E. Looney *et al.*, *Hum. Antibodies Hybridomas* **3**, 191 (1992).
21. M. Jonker *et al.*, *Clin. Exp. Immunol.* **93**, 301 (1993).
22. Materials and methods are available as supporting material on *Science Online*.
23. E. M. Janssen *et al.*, *Nature* **421**, 852 (2003).
24. D. J. Shedlock, H. Shen, *Science* **300**, 337 (2003).
25. J. C. Sun, M. J. Bevan, *Science* **300**, 339 (2003).
26. A. L. Erickson *et al.*, *Immunity* **15**, 883 (2001).
27. K. M. Chang *et al.*, *J. Clin. Invest.* **100**, 2376 (1997).
28. Single-letter abbreviations for the amino acid residues are as follows: A, Ala; C, Cys; D, Asp; E, Glu; F, Phe; G, Gly; H, His; I, Ile; K, Lys; L, Leu; M, Met; N, Asn; P, Pro; Q, Gln; R, Arg; S, Ser; T, Thr; V, Val; W, Trp; and Y, Tyr.
29. M. A. Nowak *et al.*, *Nature* **375**, 606 (1995).
30. D. Homann, L. Teyton, M. B. Oldstone, *Nature Med.* **7**, 913 (2001).

31. Supported by Public Health service grants to C.M.W. (A147367 and AI48231) and C.M.R. (CA57973, CA85883, and AI40034) and the Greenberg Medical Research Institute. NIH contract N01 HB27091 to K.K.M. is also gratefully acknowledged. A.G. is supported by a Cancer Research Institute Postdoctoral Fellowship award. N.H.S. is the recipient of postdoctoral fellowships from the Canadian Institute for Health Research and the American Liver Foundation. We thank D. Hasselschwert and N. Smith of the New Iberia Research Center, New Iberia, LA, for outstanding veterinary support; D. Conway for superb technical assistance; and J. Stacey for critical reading of the manuscript.

Supporting Online Material
www.sciencemag.org/cgi/content/full/302/5645/659/DC1
Materials and Methods
SOM Text
Tables S1 and S2
References and Notes

3 July 2003; accepted 4 September 2003

A Cellular Framework for Gut-Looping Morphogenesis in Zebrafish

Sally Horne-Badovinac,[1] Michael Rebagliati,[2] Didier Y. R. Stainier[1]*

Many vertebrate organs adopt asymmetric positions with respect to the midline, but little is known about the cellular changes and tissue movements that occur downstream of left-right gene expression to produce this asymmetry. Here, we provide evidence that the looping of the zebrafish gut results from the asymmetric migration of the neighboring lateral plate mesoderm (LPM). Mutations that disrupt the epithelial structure of the LPM perturb this asymmetric migration and inhibit gut looping. Asymmetric LPM migration still occurs when the endoderm is ablated from the gut-looping region, suggesting that the LPM can autonomously provide a motive force for gut displacement. Finally, reducing left-sided Nodal activity randomizes the pattern of LPM migration and gut looping. These results reveal a cellular framework for the regulation of organ laterality by asymmetrically expressed genes.

Some of the most dramatic examples of asymmetric organ morphogenesis in response to left-right (L-R) positional cues (*1*–*3*) occur in the digestive system, where the liver and pancreas occupy asymmetric positions with respect to the midline and the intestine bends

and folds in a complex pattern for proper packing into the abdominal cavity. In zebrafish, the first leftward bend in the developing intestine arises through a morphogenetic process known as gut looping. All of the digestive organs in zebrafish originate from a solid rod of endodermal cells that forms at the ventral midline during mid- to late somitogenesis (*4*). Looping occurs between 26 and 30 hours postfertilization (hpf), when the region of the endodermal rod that will give rise to the esophagus, intestinal bulb, and liver curves to the left (Fig. 1, A and B).

The *heart and soul* (*has*) mutation causes striking defects in asymmetric organ morphogenesis, in which gut looping fails to occur and the liver and pancreas are both symmetrical with respect to the midline (*5*). The *has* gene encodes an atypical protein kinase C, aPKCλ (*5*, *6*), which localizes to the apical junctional complex in epithelial cells and is required for the establishment of epithelial polarity (*7*). Consistent with this function, *has* mutants show defects in the formation and maintenance of several embryonic epithelia (*5*). These observations led us to hypothesize that an epithelial tissue plays a critical role in gut looping.

To determine which epithelial tissue might affect visceral L-R morphogenesis, we examined the localization of aPKCs λ and ζ in the gut-looping region at 30 hpf (*8*). The endoderm at this stage is a compact mass of cells with little to no polarization and weak expression of aPKCs (Fig. 1, G and H). In contrast, the lateral plate mesoderm (LPM) forms a highly polarized epithelium with strong expression and apical localization of aPKCs (Fig. 1, G and H). The left and right LPM epithelia each form a U-shaped structure in which the apical side of the epithelium corresponds to the inside of the U and each arm of the U consists of either columnar or squamous cells (Fig. 1, G, H, G′, and H′). The most notable feature of the LPM epithelia, however, is that the left and right sides show a distinct asymmetry in their morphology and position. The left LPM is dorsal to the endoderm, with its columnar cells on the ventral arm of the U, whereas the right LPM is ventrolateral to the endoderm, with its columnar cells on the dorsal arm of the U (Fig. 1, G and H).

The LPM is a structure that spans the entire anterior-posterior (A-P) extent of the trunk in vertebrate embryos. Notably, we only observe these columnar cells and the asymmetric placement of the left and right sides of the LPM in the A-P region of the embryo, where gut looping will occur (Fig. 1, G and H). Posterior to the looping region, the LPM cells still express aPKCs, but the cells appear squamous and both sides of the LPM lie dorsal to the endoderm (Fig. 1I). These data show that the two sides of the LPM form columnar epithelia with morphological L-R asymmetry specifically in the A-P region where gut looping occurs.

We next examined the structure and position of the LPM at earlier times in development. Before looping, the endodermal rod lies in the midline and both sides of the LPM are symmetrical and at about the same dorsoventral level as the endodermal rod (Fig. 1E). During looping, however, the LPM undergoes an unexpected asymmetric migration: both sides of the LPM migrate medially, but the left side moves dorsal to the endoderm, whereas the right side undergoes a ventrolateral migration directly abutting the endodermal rod (Fig. 1, F to H). Notably, the morphology of the LPM is markedly asymmetric before the endoderm is displaced from the midline (Fig. 1F). The early morphological asymmetry in the LPM, combined with the close apposition of the right LPM to the endoderm throughout its migration past the midline (Fig. 1H), suggests that the LPM pushes the developing intestine to the left.

To investigate whether asymmetric migration of the LPM is required for gut looping, we examined this process in *has* and *nagie oko* (*nok*) mutants. Similar to *has*/*aPKC*λ, the *nok* gene, which encodes a membrane-associated guanylate kinase, is required for the establishment of epithelial polarity (*9*). We examined endodermal morphogenesis in *nok* mutants and found that, as in *has* mutants, the gut does not loop (Fig. 2, A to C).

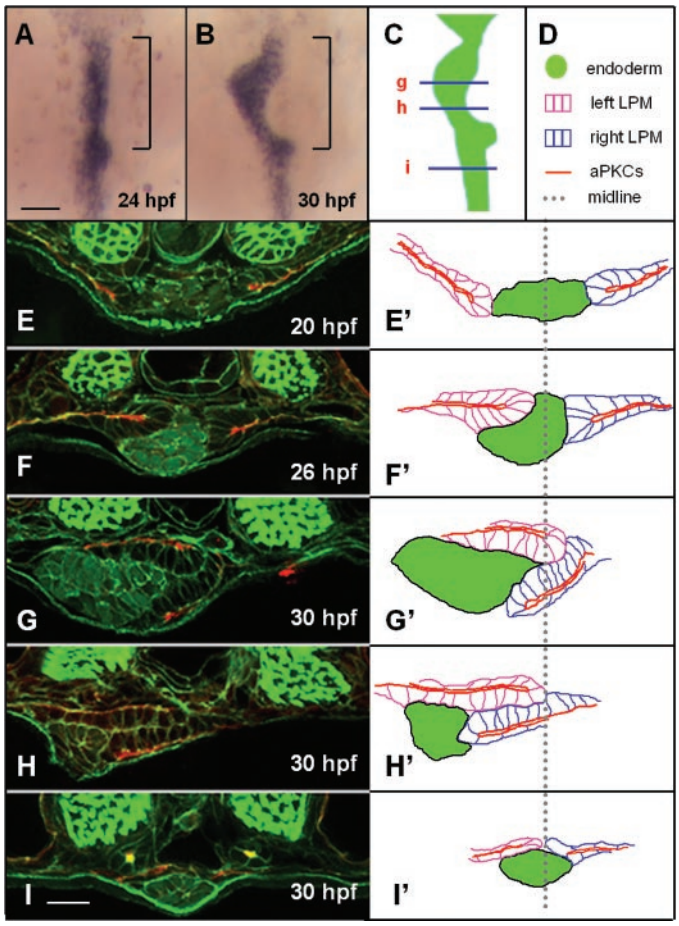

Fig. 1. The LPM undergoes asymmetric migration in the gut-looping region. (**A** and **B**) Whole-mount in situ hybridization with the endodermal marker *foxA3* reveals digestive tract morphology before (A) and immediately after (B) looping morphogenesis. Scale bar, 50 μm. The looping region (brackets) lies between the caudal border of the pharyngeal endoderm and the pancreatic islet. Dorsal views, anterior to the top. (**C**) Diagram of the looped gut at 30 hpf. Blue lines indicate position of sections in (G) to (I). (**D**) Key for the diagrams in (E′) to (I′). [(E) to (I)] Transverse sections through the endoderm and LPM. aPKCs (red) show weak expression in the endoderm but are highly expressed and apically localized in the LPM epithelium. Most cells are outlined with cortical actin (green) and endodermal cells have weak cytoplasmic green fluorescent protein (GFP). Dorsal to the top; scale bar, 20 μm. (**E**) At 20 hpf the endodermal rod lies in the midline and both sides of the LPM are at the same dorsoventral level as the endodermal rod. (**F**) At 26 hpf, both sides of the LPM have migrated medially. The left LPM is dorsal to the endoderm and the right LPM is beginning to migrate ventrolaterally. Although the LPM is markedly asymmetric at this stage, the developing intestine is still in the midline. Asymmetry seen within the endoderm is due to leftward budding of the liver, which can be genetically uncoupled from gut looping (*23*). (**G** and **H**) At 30 hpf the migration is complete. The developing intestine has shifted to the left and the position of the left versus the right LPM is highly asymmetric. (**I**) Posterior to the looping region, the LPM cells appear squamous and both sides of the LPM are dorsal to the endoderm. (**E′** to **I′**) Diagrams of the relative positions of the LPM and endoderm in confocal images [(E) to (I)].

[1]Department of Biochemistry and Biophysics, Programs in Developmental Biology, Genetics, and Human Genetics, University of California, San Francisco, CA 94143, USA. [2]Department of Anatomy and Cell Biology, Roy J. and Lucille A. Carver College of Medicine, University of Iowa, Iowa City, IA 52242, USA.

*To whom correspondence should be addressed. E-mail: didier_stainier@biochem.ucsf.edu

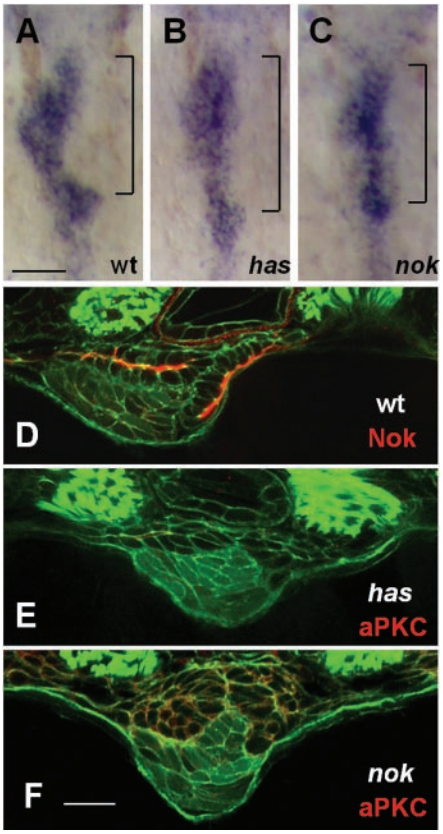

Fig. 2. Gut-looping defects in *has* and *nok* mutants. (**A** to **C**) Whole-mount in situ hybridization with *foxA3* reveals digestive tract morphology. Dorsal views, anterior to the top; scale bar, 50 μm. In wild-type embryos (A) the gut loops to the left, whereas in *has* (B) and *nok* (C) mutants it remains medial. Brackets show the looping region. (**D** to **F**) Transverse sections through the gut-looping region, dorsal to the top; scale bar, 20 μm. Most cells are outlined with cortical actin (green) and endodermal cells contain weak cytoplasmic GFP. (D) Nok (red) is weakly expressed in the endoderm but strongly expressed and apically localized in the LPM. In *has* (E) and *nok* (F) mutants, the epithelial structure of the LPM is severely disrupted, and the right LPM fails to undergo the ventrolateral migration seen in wild-type embryos. aPKCs are in red [(E) and (F)]. Red staining is low in *has* mutants (E) as the aPKC antibody does not recognize the truncated protein encoded by $has^{m567;4}$. All images are at 30 hpf.

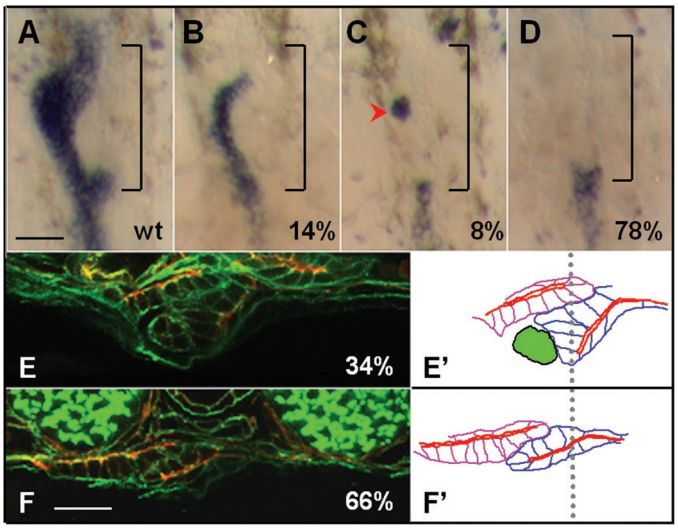

Fig. 3. Asymmetric LPM migration can occur in the absence of endoderm. (**A** to **D**) Whole-mount in situ hybridization with *foxA3*. Brackets show the gut-looping region. Dorsal views, anterior to the top; scale bar, 50 μm. (A) Wild-type embryo. [(B) to (D)] Endoderm is greatly reduced in *bon* mutants. The 74 mutants that were scored fell into three classes: (B) those with a reduced but continuous stretch of endoderm in the gut-looping region (14%); (C) those with small, discontinuous patches of endoderm (red arrowhead) in the gut-looping region (8%); and (D) those with a complete absence of endoderm in the gut-looping region (78%). (**E** and **F**) Transverse sections through the gut-looping region of *bon* mutants. Dorsal to the top; scale bar, 20 μm. Colors show actin (green) and aPKCs (red). We examined a single transverse section in 44 randomly selected *bon* mutants and found that 35 mutants (80%) showed clear asymmetric migration of the LPM past the midline. Of these 35 sections, 12 sections (34%) contained endoderm, but the amount was substantially reduced (E); 23 sections (66%) showed asymmetric LPM migration in the complete absence of endoderm (F). In 34 of the 35 sections that showed asymmetric LPM migration, the left LPM had migrated dorsal to the right LPM. (**E′** and **F′**) Diagrams of the relative positions of the LPM and endoderm in confocal images [(E) and (F)]. All images are at 30 hpf. Dotted lines mark the midline.

To assess whether the nonlooping phenotype in these mutants is due to a defect in L-R gene expression, we examined two genes that are asymmetrically expressed within the left LPM of the gut-looping region, the *Nodal* gene *southpaw* (*spaw*) (*10*) and the transcription-factor gene *pitx2* (*11*). In both *has* and *nok* mutants, *spaw* and *pitx2* expression appears normal (table S1), indicating that altered L-R gene expression does not account for the gut-looping defect.

We next examined whether the defect in gut looping was due to a defect in the morphogenetic process itself. Transverse sections through the gut-looping region in *has* and *nok* mutants revealed that the epithelial structure of the LPM is severely disrupted and that the ventrolateral migration of the right LPM is perturbed (Fig. 2, E and F). Although some cells from the right LPM move in the direction of the ventrolateral migration, the majority migrate dorsal to the endoderm (Fig. 2, E and F), similar to what is seen in nonlooping regions of the intestine (Fig. 1I). Together with the high expression of Has and Nok proteins (Figs. 1 and 2D) in the LPM during looping stages, the mutant phenotypes suggest that a defect in the LPM is responsible for the nonlooping gut phenotype observed in *has* and *nok* mutants and that the asymmetric migration of the LPM may provide the motive force for gut looping.

If the LPM does indeed displace the endoderm to the left, ablation of the looping endoderm should not affect the asymmetric migration of this tissue. Mutants for the Sox-related transcription-factor gene *casanova*, which completely lack endoderm, also have numerous defects in the migration of mesodermal tissues toward the midline (*12*). In contrast, mutants for the Mix family transcription-factor gene *bonnie and clyde* (*bon*) have a reduced number of endodermal cells (*13*) and fewer defects in mesodermal migration (*14*). We examined a single transverse section through the gut-looping region of 44 randomly selected *bon* mutants at 30 hpf and found that 35 mutants (80%) showed clear asymmetric migration of the LPM past the midline (Fig. 3, E and F). Of these 35 sections, 23 (66%) completely lacked endoderm (Fig. 3F), and in the remaining 33%, endoderm was substantially reduced (Fig. 3E). Furthermore, the left LPM was dorsal to the right LPM in 97% of the sections showing asymmetric LPM migration (Fig. 3, E and F). These data show that asymmetric migration of the LPM can occur in the absence of endoderm and suggest that the force for gut displacement is autonomous to the LPM.

To investigate whether the asymmetric migration of the LPM is dependent on normal L-R positional cues, we injected embryos with a morpholino antisense oligonucleotide (MO) (*15*, *16*) targeted against the mesoderm-specific *Nodal* gene *spaw* (*10*). MO reduction of *spaw* function abolishes left-specific gene expression (including *cyclops*, *lefty1*, *lefty2*, and *pitx2c*) in the LPM in 80 to 100% of injected embryos (*10*), yet, unlike the reported zebrafish mutations that affect L-R gene expression (*1*, *17*–*21*), the *spaw*-MO does not appear to disrupt developmental processes other than L-R asymmetry (*10*). Whole-mount in situ hybridization with the endodermal marker *foxA3* (*22*, *23*) revealed that gut looping is randomized in embryos injected with *spaw*-MO (*14*). More importantly, we found that injection of the *spaw*-MO randomizes LPM migration. Out of 60 injected embryos, 22 embryos showed the normal pattern of LPM migration (Fig. 4A), 25 embryos showed a reversed pattern of LPM migration (Fig. 4B), 7 embryos

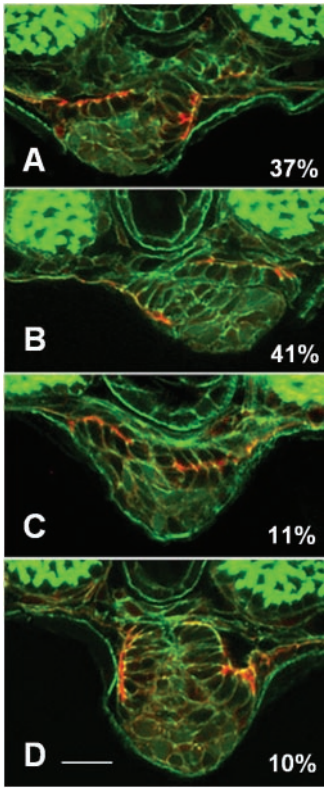

Fig. 4. Reducing *spaw* function randomizes LPM migration. Transverse sections through the gut-looping region at 30 hpf. Dorsal to the top; scale bar, 20 μm. Sections are stained as in Fig. 1. Of 60 injected embryos, 22 embryos showed the normal pattern of LPM migration: left dorsal, right ventrolateral (**A**); 25 embryos showed a reversed pattern of LPM migration: right dorsal, left ventrolateral (**B**); 7 embryos showed both sides of the LPM migrating dorsally (**C**); and 6 embryos showed both sides of the LPM migrating ventrolaterally (**D**).

showed bilateral dorsal migrations (Fig. 4C), and 6 embryos showed bilateral ventrolateral migrations (Fig. 4D). The epithelial structure of the LPM appears normal in embryos injected with *spaw*-MO (Fig. 4), indicating that it is unlikely that *has* and *nok* act as morphogenetic effectors downstream of the Nodal pathway. These data show that the pattern of LPM migration and gut looping is regulated by L-R gene expression.

Previous work on vertebrate L-R asymmetry has largely focused on signaling events that establish and pattern the L-R axis. Little is known, however, about how these L-R signals ultimately affect cell and tissue behavior to generate organ asymmetry. Our data suggest that the LPM undergoes a dynamic asymmetric migration that in turn causes the initial leftward bend in the developing intestine in zebrafish. An alternative model is that the endoderm autonomously loops to the left and the LPM follows. However, both wild-type and mutant analyses strongly suggest that the LPM provides the motive force for looping. For example, the LPM displays marked morphological asymmetry before the leftward displacement of the endoderm in wild-type embryos (Fig. 1F). Furthermore, studies with *has* and *nok* mutants show that the gut fails to loop when asymmetric migration of the LPM is perturbed, and studies with *bon* mutants show that asymmetric LPM migration can occur in the absence of endoderm. The cellular mechanisms that drive asymmetric LPM morphogenesis remain to be investigated. It is possible that the LPM epithelia are actively migratory; alternatively, the medial movement could result from concerted cell shape changes or proliferation within the plane of the epithelium. It will also be of great interest to understand how asymmetric gene expression within the LPM regulates the migration pattern of this tissue.

References and Notes

1. R. D. Burdine, A. F. Schier, *Genes Dev.* **14**, 763 (2000).
2. M. Mercola, M. Levin, *Annu. Rev. Cell Dev. Biol.* **17**, 779 (2001).
3. C. J. Tabin, K. J. Vogan, *Genes Dev.* **17**, 1 (2003).
4. E. A. Ober, H. A. Field, D. Y. Stainier, *Mech. Dev.* **120**, 5 (2003).
5. S. Horne-Badovinac *et al.*, *Curr. Biol.* **11**, 1492 (2001).
6. R. T. Peterson, J. D. Mably, J. N. Chen, M. C. Fishman, *Curr. Biol.* **11**, 1481 (2001).
7. S. Ohno, *Curr. Opin. Cell Biol.* **13**, 641 (2001).
8. Materials and methods are available as supporting material on *Science* Online.
9. X. Wei, J. Malicki, *Nature Genet.* **31**, 150 (2002).
10. S. Long, N. Ahmad, M. Rebagliati, *Development* **130**, 2303 (2003).
11. M. Campione *et al.*, *Development* **126**, 1225 (1999).
12. J. Alexander, M. Rothenberg, G. L. Henry, D. Y. Stainier, *Dev. Biol.* **215**, 343 (1999).
13. Y. Kikuchi *et al.*, *Genes Dev.* **14**, 1279 (2000).
14. S. Horne-Badovinac, D. Y. R. Stainier, data not shown.
15. J. Heasman, M. Kofron, C. Wylie, *Dev. Biol.* **222**, 124 (2000).
16. A. Nasevicius, S. C. Ekker, *Nature Genet.* **26**, 216 (2000).
17. J. N. Chen *et al.*, *Development* **124**, 4373 (1997).
18. Y. T. Yan *et al.*, *Genes Dev.* **13**, 2527 (1999).
19. B. W. Bisgrove, J. J. Essner, H. J. Yost, *Development* **127**, 3567 (2000).
20. A. J. Chin, M. Tsang, E. S. Weinberg, *Dev. Biol.* **227**, 403 (2000).
21. J. O. Liang *et al.*, *Development* **127**, 5101 (2000).
22. J. Odenthal, C. Nusslein-Volhard, *Dev. Genes Evol.* **208**, 245 (1998).
23. H. Field, E. A. Ober, T. Roeser, D. Y. Stainier, *Dev. Biol.* **253**, 279 (2003).
24. This study is dedicated to the memory of Ira Herskowitz. We thank D. Bilder, G. Martin, S. Amacher, H. Field, E. Ober, and I. Scott for discussion and critical comments on the manuscript; S. Waldron for fish care; X. Wei for the Nok antibody; and L. Trinh for homozygous *bon* mutants. Funded by the NSF and American Heart Association (S. H.-B.), a Pilot Award from the University of Iowa Diabetes and Endocrinology Research Center and the NIH (M.R.), and the Packard Foundation and NIH (D.Y.R.S.).

Supporting Online Material

www.sciencemag.org/cgi/content/full/302/5645/662/DC1
Materials and Methods
Table S1
References and Notes

7 April 2003; accepted 5 September 2003